[redacted]

Copy 205
RM L56A31

NACA RM L56A31

TECH LIBRARY KAFB, NM
0144147

Reg # 1829

NACA

RESEARCH MEMORANDUM

7677

AN EVALUATION OF AN AEROMECHANICAL METHOD OF MINIMIZING SERVO-MISSILE TRANSFER-FUNCTION VARIATIONS WITH FLIGHT CONDITION

By Martin L. Nason

Langley Aeronautical Laboratory
Langley Field, Va.

HADC
TECHNICAL LIBRARY
[redacted]

[redacted]

NATIONAL ADVISORY COMMITTEE
FOR AERONAUTICS
WASHINGTON
April 18, 1956

[redacted]

[redacted]

Classification cancelled (or changed to UNCLASSIFIED

By Authority of NASA Tech Pub Announcement #124
(OFFICER AUTHORIZED TO CHANGE)

By 10 FEB 58
NAME AND

GMR
GRADE OF OFFICER MAKING CHANGE)

28 Mar 61
DATE

TECH LIBRARY KAFB, NM
0144147

NATIONAL ADVISORY COMMITTEE FOR AERONAUTICS

RESEARCH MEMORANDUM

AN EVALUATION OF AN AEROMECHANICAL METHOD OF MINIMIZING SERVO-MISSILE TRANSFER-FUNCTION VARIATIONS WITH FLIGHT CONDITION

By Martin L. Nason

SUMMARY

A theoretical investigation has been conducted to determine the static and dynamic characteristics of a control-surface actuator and missile combination, with primary consideration being given to the minimization of the effects of Mach number and altitude. A torque-servo-controlled missile employing judicious amounts of control-surface-position feedback was found to have exceptionally favorable static and dynamic characteristics as compared with a similar missile configuration actuated by a control-surface-position servo. The control-surface-position feedback loop exhibited a strong stabilizing influence on the damping of the airframe mode and careful adjustment of the torque servo and position feedback gain constants considerably reduced the percentage variation of the available missile turning rate with Mach number and altitude. It is possible that, upon consideration of a guidance loop and tracking, this type of actuator in combination with a missile might replace a gain-adjusted acceleration control system. As a rule, this complex system employs the usual rate-gyro pitch damping loop for stabilization.

INTRODUCTION

Guided-missile control systems are plagued by variations in the airframe transfer function due to altitude and Mach number effects. Satisfactory control is usually unobtainable over the desired range of flight condition without the utilization of electronic automatic stabilization and gain-adjusting mechanisms. The inclusion of this electronic equipment tends to complicate the missile further and, therefore, results in reduced reliability. Some analytical studies have recently been undertaken in order to determine two things: (1) the effect of free-floating flaps on the pitch damping of the missile and (2) the characteristics of hinge-moment- and spring-position-actuated control surfaces on the time

rate of change of flight-path angle. (See refs. 1 and 2.) In these investigations the free-floating flap was assumed to be physically separated from the aerodynamic surfaces controlling the direction of the missile and thus the flap contributed primarily to the pitch damping. Conversely, the control surfaces were arranged so as to affect only the turning rate of the missile.

In contrast, the linear study presented herein shows how a single aerodynamic control surface and actuator can be effectively designed to perform the dual function of furnishing both improved pitch response and improved missile-turning-rate gain compensation due to Mach number and altitude effects. The analysis shows how the effect of flight condition on the steady-state missile turning rate can be minimized for a given airframe and control-surface configuration by the adjustment of only two control-surface actuator static-gain constants. Graphical plots are presented for a range of Mach numbers and altitudes which facilitate this static adjustment. Evaluation of the dynamic characteristics and stabilization of the control-surface mode was then accomplished on an electronic analog computer for the conditions of improved static gains of the system.

SYMBOLS

b	moment arm, ft
$\bar{c}$	mean aerodynamic chord, 1.776 ft
D	linear differential operator, $\frac{d}{dt}$, sec^{-1}
H	aerodynamic hinge moment acting on control surface, ft-lb
H_α	$\frac{\partial H}{\partial \alpha}$, ft-lb/radian
H_δ	$\frac{\partial H}{\partial \delta}$, ft-lb/radian
$H_{\dot{\delta}}$	$\frac{\partial H}{\partial \dot{\delta}}$, ft-lb/radian/sec (may include additional artificial damping)
I_R	moment of inertia of control surface, slug-ft^2
K_A	airframe longitudinal transfer-function coefficient, sec^{-3}

K_L proportionality constant relating control-surface deflection to position-servo ram-piston displacement, radian/in.

K_s position-servo static gain, in./r units

K_T torque-servo static-gain constant, ft-lb/r units

K_α proportionality constant between rate of change of flight path and angle of attack, sec

K_δ control-surface position feedback proportionality constant, r units/radian

k spring constant, ft-lb/radian

M Mach number

r control-surface-actuator reference input signal, r units

S control-system static gain $\left(\frac{\dot{\gamma}}{r}\right)_{ss}$, radian/sec/r units

SM airframe static margin, fraction of mean aerodynamic chord

$\frac{\Delta S}{S}$ percentage variation of system static gain (subscripts M and h denote Mach number and altitude variations, respectively)

T torque servo hinge moment acting upon control surface, ft-lb

t time, sec

x position-servo ram-piston displacement, in.

α missile angle of attack, radians

γ missile flight-path angle, radians

δ control-surface angular deflection, radians

ζ_A quadratic damping ratio of airframe, nondimensionalized constant

ζ_s quadratic damping ratio of control-surface-position servo, nondimensionalized constant

τ torque-servo transfer-function time constant, sec

ω_{n_A} undamped natural frequency of airframe, radian/sec

ω_{n_s} undamped natural frequency of control-surface-position servo, radian/sec

A dot over a symbol denotes a derivative with respect to time.

MISSILE LONGITUDINAL CONTROL

A common method of controlling the longitudinal motion of a missile is by controlling the angular position of an aerodynamic surface which when deflected produces lift and pitching moment. Aerodynamic hinge moments acting on the control surface as a result of deflection and missile angle of attack are usually overbalanced by the control-surface positioning mechanism to a sufficient degree to affect only slightly the servo output response characteristics. For borderline servo designs, in which the torque output capacity is of the order of the aerodynamic hinge moment expected, and for pneumatic systems where compressibility effects are present, coupling between the missile longitudinal and the missile control-surface motions (in addition to the intentional airframe motion feedbacks common to most conventional missile-control systems) will be produced. Experimental evidence of this coupling for a pneumatic system is reported in reference 3. In this paper, the control-surface servo will be regarded as a hinge-moment-producing device rather than as a positioning device and consideration will be given to the longitudinal coupling effects on the system response. Regarding the servo in this manner, then, the aerodynamic hinge moments, the control-surface damping, and the control-surface inertia may each be considered separately and their effects on the overall system operation can be readily ascertained.

In order to avoid confusion, the expression "torque servo" will be used to refer to a control-surface servo which programs hinge moment, and "position servo" will refer to a conventional control-surface positioning servomechanism. In addition, the term "torposervo" shall be used throughout the paper to signify a "torque servo" actuated missile employing a control-surface-position signal input into the "torque servo."

Missile Configuration and Control Surface

For analysis purposes a canard missile configuration was selected. (See fig. 1.) The longitudinal-stability derivatives were obtained from a free-flight rocket-powered test and are reported in reference 4.

The test model described in reference 4 is similar to the configuration chosen for the analysis (fig. 1) except for the control-surface design. In reference 4 the control surfaces were 60° delta surfaces. Aerodynamic hinge moments on the control surfaces shown in figure 1 were obtained from experimental wind-tunnel measurements (unpublished). In order to insure that the longitudinal-stability derivatives reported in reference 4 would be valid, the area of the wind-tunnel test control surfaces was rescaled to equal the area of the 60° delta control surfaces. The position of the control surface shown in figure 1 was arbitrarily placed 0.3 inch forward of those tested in reference 4 to account for the increased angle of sweepback of both the leading and trailing edges. The longitudinal-transfer-function coefficients and hinge-moment parameters are tabulated in table I for the range of flight conditions and static margins investigated herein.

Torposervo and Position-Servo System Block Diagrams

Shown in figure 2, in block diagram form, is a torposervo-actuated missile with the torque servo represented by a proportional gain K_T and a time constant τ. The control-surface dynamics are assumed to be characterized by a second-order transfer function with the control-surface inertia I_R; damping $H_{\dot{\delta}}$; and aerodynamic hinge-moment parameter H_δ terms present. Conventional, linearized two-degree-of-freedom longitudinal dynamics were utilized in the derivation of the $\frac{\dot{\gamma}}{\delta}$ and $\frac{\alpha}{\dot{\gamma}}$ transfer functions. A feedback loop around the airframe and control-surface blocks is necessary to simulate the aerodynamic hinge moment H_α on the control surface due to missile angle of attack α. The input signal r is considered to be the command signal to the control system which would necessarily be furnished by the seeker or missile guidance system.

A block diagram of a position-servo-actuated missile is also shown in figure 2 for comparison purposes. The control-surface-position-servo transfer function is assumed to be of the second order and has a mechanical linkage with a proportionality constant K_L which relates the control-surface rotation δ to the translation x of the servo ram piston. It should be noted that no airframe feedback signals are indicated, thus making the motion of the control surface and airframe a function only of the servo input signal r.

Torposervo Control-Surface Dynamic Considerations

If the natural frequency of the missile is significantly lower than that of the control surface, it can be expected that the high-frequency

oscillations of the control surface will affect only slightly the missile mode of motion. Physically, this means that the motion of the control surface will be determined essentially by the static aerodynamic and torque servo moments acting upon it and, consequently, will follow approximately the motion of the missile. Preliminary studies of system dynamics in which the control-surface inertia reaction moment $I_R\ddot{\delta}$ and control-surface damping moment $H_{\dot{\delta}}\dot{\delta}$ terms were set equal to zero indicated this reasoning to be valid; however, these terms were included in the analysis because of the occurrence of high-frequency control-surface mode instabilities at small values of control-surface damping. The pitch inertia reaction moment $I_R\ddot{\theta}$ on the control surface was found to be negligible for the determination of either the control surface or airframe motion and was disregarded throughout the study.

DESIGN APPROACH EMPLOYED FOR THE MINIMIZATION OF FLIGHT CONDITION EFFECTS

The primary objective of this analysis is to minimize, if possible, the transfer-function variations with Mach number and altitude. In general, the variation of the static gain of the servo and airframe combination with flight condition is usually more troublesome from the standpoint of attaining satisfactory overall guidance-system operation than are the changes in damping and natural frequency of the airframe. In view of this situation it was decided to concentrate effort on first obtaining improvements in the static gain variations with flight condition and second on examining the dynamic response characteristics for the conditions of improved static gain.

The steady-state expresions relating the time rate of change of flight-path angle $\dot{\gamma}$ to a constant input signal r for the torposervo and position-servo-actuated missile, respectively (see fig. 2) are given as follows for a controls-forward missile configuration.

For the torposervo,

$$S = \frac{K_T}{-K_\alpha H_\alpha + \frac{\omega_{nA}^2}{K_A}\left(K_T K_\delta - H_\delta\right)} \tag{1}$$

For the position servo,

$$S = K_s K_L \frac{K_A}{\omega_{n_A}^2} \tag{2}$$

A preliminary study of the static gain S established the fact that for a torque-servo-actuated missile $\left(\text{torposervo with } K_\delta = 0\right)$ the trend of the system static gain with Mach number and altitude is opposite to that trend existing for a position-servo-actuated missile. In figure 3 is shown a typical plot of the system static gain S for a torque-servo- and position-servo-actuated missile. This trend implies that if, somehow, the static properties of a torque and position servo could be combined, then a hybrid system might evolve that would possess some of the advantages of both types of control considered from the standpoint of minimum flight condition effects. Since a very strong position feedback signal around a torque servo (see fig. 2) would essentially reduce the torque servo to a position servo, it was reasoned that a comparatively weak position feedback signal might have the desirable static characteristics being sought. This is the reason for the inclusion of the control-surface-position feedback loop and the basis for the evolution of the torposervo becomes evident.

Fortunately, some system parameters do exist which, when changed, cause only modifications to the dynamic response and thus do not need to be considered for static studies. For example, neither the control-surface damping H_δ nor the torque-servo time constant τ appears in equation (1). Therefore, these quantities may be temporarily neglected for the static study and later set upon evaluation of the dynamic response characteristics.

No variations in the shape, size, or mass of the airframe or control surfaces were considered, and the longitudinal-transfer-function coefficients and control-surface-hinge-moment parameters tabulated in table I were used in all calculations. Of course, this implies that the airframe and control surfaces chosen are very probably not an optimum combination for the minimization of static gain variation; however, a major factor in the selection of the missile configuration was the existence of reliable experimental data.

Selection of the airframe and control-surface configuration specifies all the parameters in equation (1) except K_T and K_δ. Consequently, these gains may be considered to be the design variables for system static considerations. In order to compute the effect of the gains K_T and K_δ

on the variation of the system static gain S readily, percentage variations were calculated for the torposervo- and position-servo-actuated missile according to the following relationships:

For the torposervo,

$$\left(\frac{\Delta S}{S}\right)_M = \left[\frac{(S)_{M=2.0} - (S)_{M=1.2}}{(S)_{M=1.2}}\right]100 \tag{3}$$

$$\left(\frac{\Delta S}{S}\right)_h = \left[\frac{(S)_{h=40,000} - (S)_{h=0}}{(S)_{h=40,000}}\right]100 \tag{4}$$

For the position servo,

$$\left(\frac{\Delta S}{S}\right)_M = \left[\frac{(S)_{M=2.0} - (S)_{M=1.2}}{(S)_{M=2.0}}\right]100 \tag{5}$$

$$\left(\frac{\Delta S}{S}\right)_h = \left[\frac{(S)_{h=40,000} - (S)_{h=0}}{(S)_{h=0}}\right]100 \tag{6}$$

Plots of $\left(\frac{\Delta S}{S}\right)_M$ against altitude and $\left(\frac{\Delta S}{S}\right)_h$ against Mach number for various values of the static gain K_T and K_δ will then allow visual evaluation of the system static gain variation over a range of flight conditions.

In order to investigate the dynamic response characteristics of the torposervo- and position-servo-actuated missiles, an electronic analog simulation of the block diagrams shown in figure 2 was performed utilizing the combination of the static gains K_T and K_δ yielding near minimum $\left(\frac{\Delta S}{S}\right)_M$ and $\left(\frac{\Delta S}{S}\right)_h$, respectively. The time history of the rate of change of flight path $\dot{\gamma}$ subsequent to a unit step input signal ($r = 1.0$ for $t > 0$) was recorded for a number of conditions. The simulation was conducted in a manner allowing the control-surface actuator and control-surface dynamic characteristics to be varied to facilitate study of their

individual effects. In the appendix the transfer-function for a torposervo-actuated missile system is given relating the system ouput response $\dot{\gamma}$ to the actuator input signal r.

RESULTS AND DISCUSSION

Since the servo static gain and the control-surface-position-feedback constant were initially determined prior to the consideration of dynamic effects, the evaluation of the static characteristics will be discussed before the examination of the analog simulator results. This permits a logical, sequential development of the results in accordance with the analysis procedure adopted.

Control-System Static Characteristics

Values of equation (1) were computed for a range of flight conditions, torque-servo gains K_T and position-feedback gains K_δ. These are tabulated in table II. Equation (2) was also computed for a range of flight conditions with $K_S K_L$ arbitrarily set equal to 1. These are tabulated in table III.

Plots of the percentage variation of S based on equations (3) to (6) against K_T and K_δ are shown in figures 4, 5, and 6 for two static margins and a range of Mach numbers and altitudes. The variations for the position servo (eqs. (5) and (6)) are based upon a Mach number of 2.0 at sea level, rather than on a Mach number of 1.2 at 40,000 feet as was done for the torposervo (eqs. (3) and (4)), because opposite trends of the system static gain S with flight conditions are experienced and a fairer comparison is achieved by this method. For a given flight condition and static margin all the parameters necessary to determine S for a torposervo-actuated missile are specified by the previous selection of the airframe and control-surface configuration with the exception of K_T and K_δ. Therefore, figures 4 and 5 may be considered to be design plots from which satisfactory setting of K_T and K_δ can be selected. This selection achieves acceptable percentage varitions of S for a given range of flight conditions and static margins.

For a torposervo-actuated missile, figures 4 and 5 show that, as the servo static gain K_T is increased, the system is more sensitive to variations in position-feedback gain K_δ, and also that the trend in percentage variations with increasing K_δ is opposite for Mach numbers and altitude changes. Nevertheless, the trend of the percentage variations

with both Mach number and altitude for any combination of K_T and K_δ are the same. Comparison of figures 4 and 5 with figure 6 reveals that a combination of K_T and K_δ may be selected so that the percentage variation of the system static gain with either Mach number or altitude for a torposervo-actuated missile is less than that for a position-servo-actuated missile for both large and small airframe static margins. It is also possible to attain improvements for both Mach number and altitude variations simultaneously with either a large or a small static margin; however, a sacrifice is generally made in the smallest percentage variation due to Mach number or altitude attainable for the system.

In table IV is listed a set of K_T and K_δ gain constant combinations which yield near-minimum Mach number and altitude variations for the two static margins investigated. It is interesting to note that the torque-servo gain constant settings are nearly the same magnitude for the two static margins considered; however, the amounts of position-feedback gain required in each case are very different. In figure 7 are shown plots of the torposervo-actuated-missile-system static gain S against Mach number and altitude for the K_T and K_δ gain settings tabulated in table IV. These graphs were plotted for the extreme values of the Mach number and altitude ranges investigated. The variation of S with either Mach number or altitude is small for the conditions shown.

Control-System Dynamic Characteristics

The evaluation of the dynamic qualities of the system is based primarily on visual examination of the analog simulator transient time histories. The transient response characteristics of a linear system, such as damping and frequency, are determined by the roots of the system characteristic equation. For the torposervo a fifth-order characteristic equation results (see appendix) and can be considered to be equivalent to two quadratic factors representing the control surface and airframe modes of motion and a first-order factor typifying the torque servo mode. Examination of the coefficients of the torposervo system characteristic equation indicates that the static design parameters K_T and K_δ always appear as a product; thus, a variation of either parameter will be dynamically equivalent to a proportional variation of the other.

Whenever the expression "damping" is used in either the control-surface or airframe mode it will refer to the magnitude of the real part of the complex root representing that particular mode.

Effect of Mach number, altitude, and static margin.- In figures 8 and 9 the torposervo system transient responses are shown for the gain settings tabulated in table IV (gain settings corresponding to minimum

Mach number and altitude percentage variations) for three Mach numbers, two altitudes, and two airframe static margins. The control-surface damping rate was set equal to -0.4 and -0.6 ft-lb/radian/sec for the small and large static margins, respectively. The control-surface inertia remained constant for all runs at 0.01 slug-ft^2. A value of 0.1 second was selected for the torque servo time constant τ on the basis of being physically attainable in an actual torque servo design. This quantity also remained constant throughout the runs plotted in figures 8 and 9. In all cases considered (figs. 8 and 9), the system exhibited positive damping for all modes. The airframe mode dominated the motion in the system response. An increase in Mach number causes a slight increase in the airframe mode oscillation frequency at sea level and at 40,000 feet for both the small and large static margins. However, for the large static margin at 40,000 feet the damping of the airframe mode is poor for the minimum percentage altitude gain adjustment $\left(K_T = 0.3,\ K_\delta = 57.3\right)$. In general, response times (time to reach and remain within 5 percent of steady state) less than 0.7 second at sea level and less than 2.0 seconds at 40,000 feet can be obtained by proper adjustment of the system gains.

The effect of control-surface damping $H_{\dot{\delta}}$.- Plots are shown in figure 10 of the torposervo transient responses for three values of control-surface damping $H_{\dot{\delta}}$. When the control-surface damping is zero, the control-surface mode is dynamically unstable (high-frequency divergent oscillation existing in transient time history) for both sea level and 40,000 feet altitudes. The addition of control-surface damping corresponding to -0.05 ft-lb/radian/sec eliminates this objectionable instability at sea level but not at 40,000 feet. Increasing the damping to -0.20 ft-lb/radian/sec completely stabilizes the control-surface mode at both altitudes. It is significant, however, to observe the small effect of control-surface damping on either the damping or frequency of the airframe mode at the two altitudes considered.

The effect of control-surface-position feedback K_δ.- In order to ascertain the dynamic effects of the addition of a control-surface-position-feedback loop the gain constant K_δ was allowed to undergo changes and the system response recorded for each change. This study is illustrated by time-history plots of $\dot{\gamma}$ shown in figure 11 for three values of K_δ. As the amount of position feedback is increased from 0 to 114.6r units/radian, the damping of the airframe mode is greatly improved at 40,000 feet; however, only a slight change was evident at sea level. Apparently, this parameter K_δ has a strong influence over the phase relationship between the airframe and control-surface motions and, consequently, should receive careful attention for both static and dynamic studies of torposervo actuated missiles, since its adjustment can yield beneficial effects on the overall system response.

Effect of torque-servo time constant τ.- In figure 12 analog computer simulation records have been reproduced showing the effect of the torque-servo time constant τ. The time constant was increased and responses taken at three separate values. In general, the effect of the increase in time constant was to slow down the rate at which the transient approached its steady-state value. No apparent effect on the relative stability of the primary oscillatory modes is present as evidenced by any significant modifications to the damping or frequency of same.

Comparison of Torposervo and Position-Servo Actuation

Analog computer records are shown in figure 13 for the position-servo-actuated missile for a range of flight conditions and airframe static margins. For all cases a control-surface servo, which had a damping ratio ζ_s, of 0.5 and an undamped natural frequency ω_{n_s} of 60 radians per second, was assumed. A unit input signal r was utilized and $K_s K_L$ was arbitrarily set equal to 1 in all the runs. A qualitative inspection of these transient responses reveals the conventional trends of the airframe short-period mode damping and frequency variations usually experienced with Mach number, altitude, and static margin. Comparison of figures 13(a) and 13(b) with figures 8 and 9, respectively, indicates that a torposervo-actuated missile with appropriate amounts of position feedback is far superior, from a dynamic standpoint, to a position-servo-actuated missile for either a small or large static margin. In all cases, the oscillation frequency of the dominant mode in the torpo-servo control system was higher than the short-period two-degree-of-freedom airframe mode. Evidently, this can be attributed to the free-floating action of the torposervo-actuated control surface when coupled with the airframe motion. This tendency of the airframe frequency mode to increase for forward free-floating control surfaces was predicted in reference 1. A consequence of the higher frequency and also the improved damping of the airframe mode caused by the control-surface-position feed-back is a reduction in the system response time.

Additional Remarks and Suggestions for Future Research

A system whose functioning approximates that of a torposervo and allows use of conventional control-surface positioning equipment is shown in figure 14. This system is similar to the one investigated in reference 2 except for the position-feedback loop. In this system a linear spring has been inserted between the output shaft of a position servo and the control surface. The system static gain for this type of control is given as follows:

$$S = \frac{K_s \frac{k}{b}}{-K_\alpha H_\alpha + \frac{\omega_{n_A}^2}{K_A}\left(K_s K_\delta \frac{k}{b} + k - H_\delta\right)} \tag{7}$$

Although this particular system as such received no study herein, it is presented as a possible alternative design which might actually be undertaken if the system parameters allow proper adjustment of gain and spring constants.

Some consideration was given to the static characteristics of a torque-servo-actuated control-aft arrangement. A forward hinge-line location was chosen which yielded a statically stable control surface: negative H_δ and H_α. This arrangement caused extremely sensitive pitch control and irregular large magnitude variations of the overall servo and missile static gain with Mach number and altitude. This was primarily due to the cancellation of aerodynamic hinge moments caused by control-surface deflection and angle of attack since for a control-aft arrangement positive control deflection caused a negative angle of attack. Therefore, only missile configurations actuated by forward control surfaces were seriously studied; however, a more intensive study might reveal some useful properties of a control-aft arrangement.

CONCLUSIONS

The combined static and dynamic operating characteristics of a control-surface actuator and missile configuration have been investigated, with primary consideration being given to the minimization of the effects of Mach number and altitude. A torque servo employing judicious amounts of control-surface position feedback, designated herein as a torposervo, was found to have exceptionally favorable operating characteristics, and, thus, was of major interest in this investigation. Judgment of the torposervo-actuated missile was based upon comparison with a similar missile configuration actuated by a control-surface-position servo. From the results of this study the following conclusions can be made:

1. In general, the static gain variation with flight condition and the damping and frequency characteristics of a torposervo-actuated missile are far superior to those of a control-surface-position-actuated missile. It is possible that this superiority would allow replacement of a gain adjusted acceleration control system, with rate-gyro pitch damping, by an inexpensive, simple torposervo system.

2. The control-surface-position feedback loop exhibited dynamically a strong stabilizing influence in that the damping of the airframe mode

during torposervo actuation was significantly improved by its addition to the system.

3. The presence of control-surface damping was found to be mandatory to maintain dynamic stability of the control-surface mode; however, the addition of control-surface damping had an insignificant effect on the damping or frequency of the airframe mode of oscillation during torposervo actuation.

Langley Aeronautical Laboratory,
National Advisory Committee for Aeronautics,
Langley Field, Va., January 16, 1956.

APPENDIX

TRANSFER FUNCTION FOR A TORPOSERVO-ACTUATED MISSILE

The transfer function relating the rate of change of flight path, $\dot{\gamma}$, to the input signal r for a torposervo-actuated missile is given below.

$$\frac{\dot{\gamma}}{r} = \frac{b_1}{a_5D^5 + a_4D^4 + a_3D^3 + a_2D^2 + a_1D + a_0}$$

where

$$a_5 = \tau I_R$$

$$a_4 = \tau\left(2\zeta_A\omega_{n_A}I_R - H_{\dot{\delta}}\right) + I_R$$

$$a_3 = \tau\left(I_R\omega_{n_A}{}^2 - 2\zeta_A\omega_{n_A}H_{\dot{\delta}} - H_\delta\right) + \left(2\zeta_A\omega_{n_A}I_R - H_{\dot{\delta}}\right)$$

$$a_2 = \tau\left(-2\zeta_A\omega_{n_A}H_\delta - H_{\dot{\delta}}\omega_{n_A}{}^2\right) + \left(I_R\omega_{n_A}{}^2 - 2\zeta_A\omega_{n_A}H_{\dot{\delta}} - H_\delta\right) + K_TK_\delta$$

$$a_1 = -H_\delta\left(\tau\omega_{n_A}{}^2 + 2\zeta_A\omega_{n_A}\right) - H_{\dot{\delta}}\omega_{n_A}{}^2 + 2\zeta_A\omega_{n_A}K_TK_\delta - K_A\tau K_\alpha H_\alpha$$

$$a_0 = \omega_{n_A}{}^2\left(K_TK_\delta - H_\delta\right) - K_AK_\alpha H_\alpha$$

and

$$b_1 = K_AK_T$$

REFERENCES

1. Clements, James E.: A Theoretical Analysis of a Simple Aerodynamic Device To Improve the Longitudinal Damping of a Cruciform Missile Configuration at Supersonic Speeds. NACA RM L55H31, 1955.

2. Hikido, Katsumi, Hayashi, Paul H., and Lessing, Henry C.: Investigations of the Effect on Missile Dynamics of Aerodynamic and Mechanical Devices Designed for the Simplification of Missile Guidance Systems. NACA RM A55L09, 1956.

3. Seaberg, Ernest C., Sproull, Royce H., and Reid, H. J. E., Jr.: Flight Investigation at Supersonic Mach Numbers of an Automatic Acceleration Control Missile in Which Rate Damping is Obtained From a Linear Accelerometer Placed Ahead of the Missile Center of Gravity. NACA RM L55G29, 1955.

4. Zarovsky, Jacob, and Gardiner, Robert A.: Flight Investigation of a Roll-Stabilized Missile Configuration at Varying Angles of Attack at Mach Numbers Between 0.8 and 1.79. NACA RM L50H21, 1951.

TABLE I

AIRFRAME AND CONTROL-SURFACE CHARACTERISTICS

Static margin (M = 1.6)	Altitude, ft	Mach number	$2\zeta_A\omega_{n_A}$	$\omega_{n_A}^2$	K_A	K_α	H_δ, $\frac{\text{ft-lb}}{\text{rad}}$	H_α, $\frac{\text{ft-lb}}{\text{rad}}$
$-0.094\bar{c}$	Sea level	1.2	6.44	209	1580	0.256	-203	-265
	Sea level	1.6	7.76	230	2800	.222	-299	-406
	Sea level	2.0	9.29	164	4180	.191	-387	-567
	20,000	1.2	3.31	94.7	363	.517	-94.1	-122
	20,000	1.6	3.84	103	638	.448	-137	-187
	20,000	2.0	4.62	71.7	957	.381	-179	-262
	40,000	1.2	1.41	37.3	61.6	1.214	-37.7	-49.1
	40,000	1.6	1.65	40.6	110	1.044	-54.8	-74.8
	40,000	2.0	1.99	27.4	167	.883	-71.9	-105
$-0.564\bar{c}$	Sea level	1.2	7.16	919	1580	0.256	-203	-265
	Sea level	1.6	8.64	1318	2800	.222	-299	-406
	Sea level	2.0	9.80	1789	4180	.191	-387	-567
	20,000	1.2	3.54	422	363	.517	-94.1	-122
	20,000	1.6	4.26	602	638	.448	-137	-187
	20,000	2.0	4.87	816	957	.381	-179	-262
	40,000	1.2	1.51	167	61.6	1.214	-37.7	-49.1
	40,000	1.6	1.84	241	110	1.044	-54.8	-74.8
	40,000	2.0	2.10	325	167	.883	-71.9	-105

TABLE II

TABULATION OF TORPOSERVO-ACTUATED-MISSILE STATIC GAINS

Altitude, ft	Static margin (M = 1.6)	Mach number	K_S, r units/radian	K_T, ft-lb/r units	S, Radians/sec / r units
Sea level	0.094$\bar{c}$	1.2	0	0.2	0.00211
			0	.4	.00422
			0	.7	.00739
			0	1.0	.0106
			57.3	.2	.00208
			57.3	.4	.00409
			57.3	.7	.00700
			57.3	1.0	.00978
			114.6	.2	.00205
			114.6	.4	.00397
			114.6	.7	.00665
			114.6	1.0	.00910
Sea level	0.094$\bar{c}$	1.6	0	0.2	0.00174
			0	.4	.00349
			0	.7	.00610
			0	1.0	.00872
			57.3	.2	.00173
			57.3	.4	.00343
			57.3	.7	.00593
			57.3	1.0	.00838
			114.6	.2	.00172
			114.6	.4	.00338
			114.6	.7	.00577
			114.6	1.0	.00806
Sea level	0.094$\bar{c}$	2.0	0	0.2	0.00162
			0	.4	.00324
			0	.7	.00567
			0	1.0	.00810
			57.3	.2	.00161
			57.3	.4	.00322
			57.3	.7	.00560
			57.3	1.0	.00795
			114.6	.2	.00161
			114.6	.4	.00319
			114.6	.7	.00553
			114.6	1.0	.00781
Sea level	0.564$\bar{c}$	1.2	0	0.3	0.00161
			0	.4	.00215
			0	.7	.00377
			0	1.0	.00538
			57.3	.3	.00153
			57.3	.4	.00201
			57.3	.7	.00335
			57.3	1.0	.00456
			229.2	.3	.00133
			229.2	.4	.00167
			229.2	.7	.00251
			229.2	1.0	.00313

TABLE II.- Continued

TABULATION OF TORPOSERVO-ACTUATED-MISSILE STATIC GAINS

Altitude, ft	Static margin (M = 1.6)	Mach number	K_δ, r units/radian	K_T, ft-lb/r units	S, Radians/sec / r units
Sea level	0.564$\bar{c}$	1.6	0	0.3	0.00130
			0	.4	.00173
			0	.7	.00303
			0	1.0	.00433
			57.3	.3	.00126
			57.3	.4	.00166
			57.3	.7	.00280
			57.3	1.0	.00388
			229.2	.3	.00114
			229.2	.4	.00146
			229.2	.7	.00229
			229.2	1.0	.00295
Sea level	0.564$\bar{c}$	2.0	0	0.3	0.00110
			0	.4	.00146
			0	.7	.00256
			0	1.0	.00365
			57.3	.3	.00107
			57.3	.4	.00141
			57.3	.7	.00241
			57.3	1.0	.00335
			229.2	.3	.000989
			229.2	.4	.00128
			229.2	.7	.00204
			229.2	1.0	.00269
20,000	0.94$\bar{c}$	1.2	0	0.2	0.00228
			0	.4	.00457
			0	.7	.00799
			0	1.0	.0114
			57.3	.2	.00221
			57.3	.4	.00427
			57.3	.7	.00714
			57.3	1.0	.00975
			114.6	.2	.00214
			114.6	.4	.00402
			114.6	.7	.00645
			114.6	1.0	.00851
20,000	0.094$\bar{c}$	1.6	0	0.2	0.00189
			0	.4	.00378
			0	.7	.00661
			0	1.0	.00944
			57.3	.2	.00186
			57.3	.4	.00365
			57.3	.7	.00623
			57.3	1.0	.00869
			114.6	.2	.00183
			114.6	.4	.00353
			114.6	.7	.00589
			114.6	1.0	.00804

TABLE II.- Continued

TABULATION OF TORPOSERVO-ACTUATED-MISSILE STATIC GAINS

Altitude, ft	Static margin (M = 1.6)	Mach number	K_δ, r units/radian	K_T, ft-lb/r units	S, Radians/sec / r units
20,000	0.094$\bar{c}$	2.0	0	0.2	0.00177
			0	.4	.00353
			0	.7	.00618
			0	1.0	.00883
			57.3	.2	.00175
			57.3	.4	.00348
			57.3	.7	.00602
			57.3	1.0	.00851
			114.6	.2	.00174
			114.6	.4	.00343
			114.6	.7	.00587
			114.6	1.0	.00821
20,000	0.564$\bar{c}$	1.2	0	0.3	0.00174
			0	.4	.00232
			0	.7	.00406
			0	1.0	.00580
			57.3	.3	.00156
			57.3	.4	.00201
			57.3	.7	.00319
			57.3	1.0	.00418
			229.2	.3	.00119
			229.2	.4	.00143
			229.2	.7	.00195
			229.2	1.0	.00228
20,000	0.564$\bar{c}$	1.6	0	0.3	0.00141
			0	.4	.00188
			0	.7	.00329
			0	1.0	.00469
			57.3	.3	.00131
			57.3	.4	.00170
			57.3	.7	.00279
			57.3	1.0	.00374
			229.2	.3	.00108
			229.2	.4	.00134
			229.2	.7	.00192
			229.2	1.0	.00233
20,000	0.564$\bar{c}$	2.0	0	0.3	0.00119
			0	.4	.00158
			0	.7	.00277
			0	1.0	.00396
			57.3	.3	.00112
			57.3	.4	.00147
			57.3	.7	.00244
			57.3	1.0	.00332
			229.2	.3	.000964
			229.2	.4	.00121
			229.2	.7	.00180
			229.2	1.0	.00223

TABLE II.- Continued

TABULATION OF TORPOSERVO-ACTUATED-MISSILE STATIC GAINS

Altitude ft	Static margin (M = 1.6)	Mach number	K_δ, r units/radian	K_T, ft-lb/r units	$\frac{\dot{S}, \text{Radians/sec}}{\text{r units}}$
40,000	0.094$\bar{c}$	1.2	0	0.2	0.00243
			0	.4	.00485
			0	.7	.00849
			0	1.0	.01213
			57.3	.2	.00224
			57.3	.4	.00415
			57.3	.7	.00656
			57.3	1.0	.00854
			114.6	.2	.00208
			114.6	.4	.00363
			114.6	.7	.00534
			114.6	1.0	.00659
40,000	0.094$\bar{c}$	1.6	0	0.2	0.00203
			0	.4	.00407
			0	.7	.00712
			0	1.0	.0102
			57.3	.2	.00195
			57.3	.4	.00375
			57.3	.7	.00619
			57.3	1.0	.00837
			114.6	.2	.00187
			114.6	.4	.00347
			114.6	.7	.00547
			114.6	1.0	.00711
40,000	0.094$\bar{c}$	2.0	0	0.2	0.00191
			0	.4	.00383
			0	.7	.00670
			0	1.0	.00957
			57.3	.2	.00188
			57.3	.4	.00369
			57.3	.7	.00630
			57.3	1.0	.00878
			114.6	.2	.00185
			114.6	.4	.00357
			114.6	.7	.00595
			114.6	1.0	.00811
40,000	0.564$\bar{c}$	1.2	0	0.3	0.00185
			0	.4	.00247
			0	.7	.00433
			0	1.0	.00618
			57.3	.3	.00144
			57.3	.4	.00179
			57.3	.7	.00259
			57.3	1.0	.00315
			229.2	.3	.000862
			229.2	.4	.000975
			229.2	.7	.00117
			229.2	1.0	.00128

TABLE II.- Concluded

TABULATION OF TORPOSERVO-ACTUATED-MISSILE STATIC GAINS

Altitude, ft	Static margin (M = 1.6)	Mach number	K_δ, r units/radian	K_T, ft-lb/r unit	S, Radians/sec / r units
40,000	$0.564\bar{c}$	1.6	0	0.3	0.00151
			0	.4	.00202
			0	.7	.00353
			0	1.0	.00505
			57.3	.3	.00127
			57.3	.4	.00161
			57.3	.7	.00245
			57.3	1.0	.00309
			229.2	.3	.000860
			229.2	.4	.00118
			229.2	.7	.00127
			229.2	1.0	.00143
40,000	$0.564\bar{c}$	2.0	0	0.3	0.00129
			0	.4	.00172
			0	.7	.00301
			0	1.0	.00430
			57.3	.3	.00113
			57.3	.4	.00144
			57.3	.7	.00225
			57.3	1.0	.00291
			229.2	.3	.000819
			229.2	.4	.000973
			229.2	.7	.00129
			229.2	1.0	.00147

TABLE III

TABULATION OF POSITION-SERVO-ACTUATED MISSILE STATIC GAINS

Altitude, ft	Static margin (M = 1.6)	Mach number	$K_B K_L$, radians/r units	S, Radians/sec / r units
Sea level	$0.094\bar{c}$	1.2	1.0	7.56
	$0.094\bar{c}$	1.6		12.12
	$0.094\bar{c}$	2.0		25.55
	$0.564\bar{c}$	1.2		1.73
	$0.564\bar{c}$	1.6		2.12
	$0.564\bar{c}$	2.0		2.34
20,000	$0.094\bar{c}$	1.2	1.0	3.83
	$0.094\bar{c}$	1.6		6.19
	$0.094\bar{c}$	2.0		13.46
	$0.564\bar{c}$	1.2		.860
	$0.564\bar{c}$	1.6		1.06
	$0.564\bar{c}$	2.0		1.17
40,000	$0.094\bar{c}$	1.2	1.0	1.65
	$0.094\bar{c}$	1.6		2.71
	$0.094\bar{c}$	2.0		6.08
	$0.564\bar{c}$	1.2		.368
	$0.564\bar{c}$	1.6		.458
	$0.564\bar{c}$	2.0		.513

TABLE IV

SUMMARY OF STATIC GAIN ADJUSTMENTS

Static margin (M = 1.6)	K_δ, r units/radian	K_T, ft-lb/r units	Description
$0.094\bar{c}$	57.3 114.6	1 0.4	Minimum Mach number variation Minimum altitude variation
$0.564\bar{c}$	229.2 57.3	1 0.3	Minimum Mach number variation Minimum altitude variation

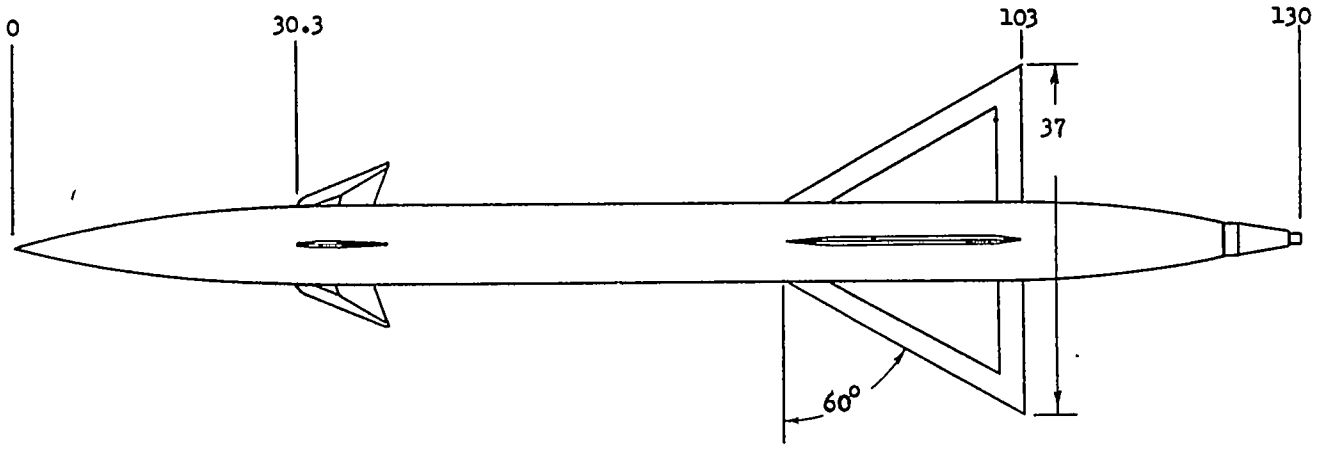

(a) Airframe.

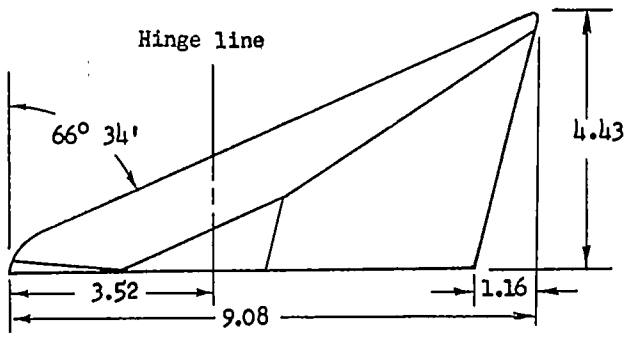

(b) Control surface.

Figure 1.- Sketch of missile configuration and control-surface plan form. All dimensions indicated are in inches.

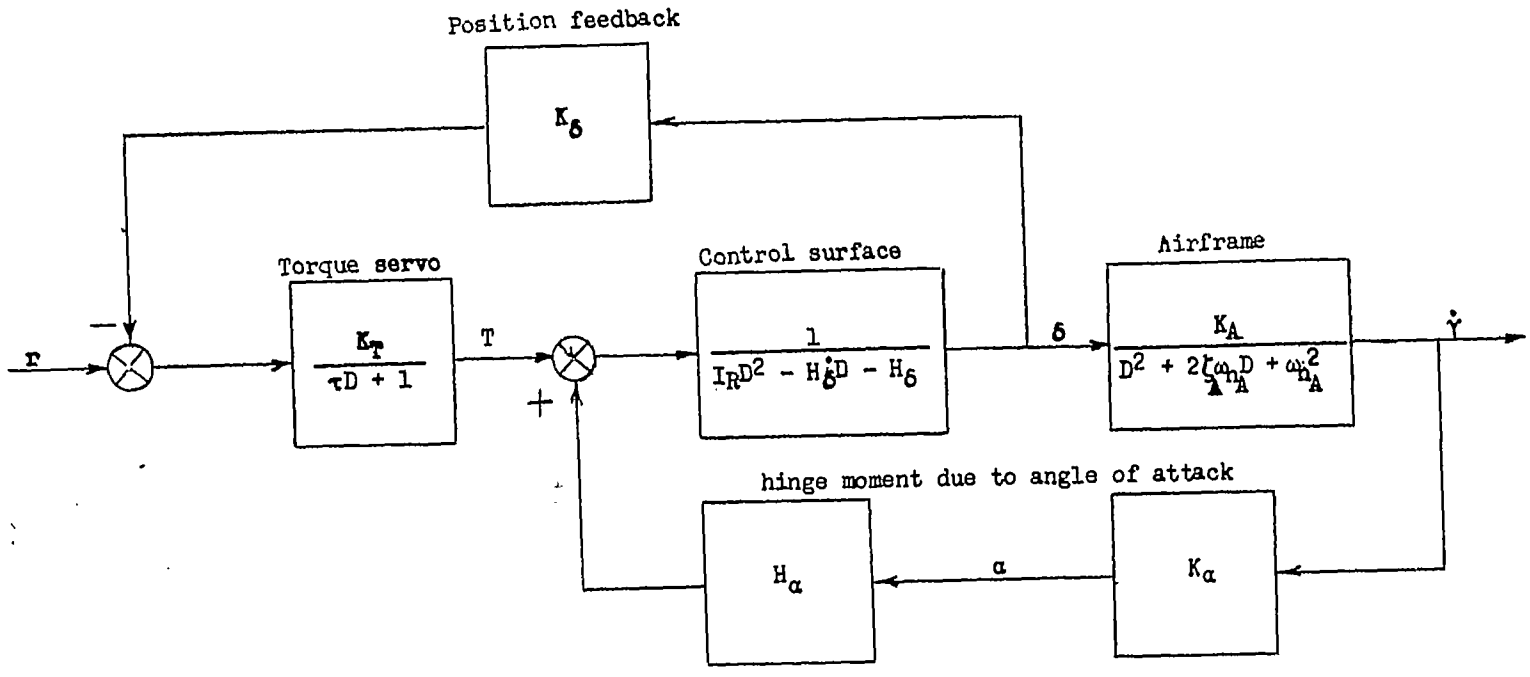

(a) Torposervo-actuated missile.

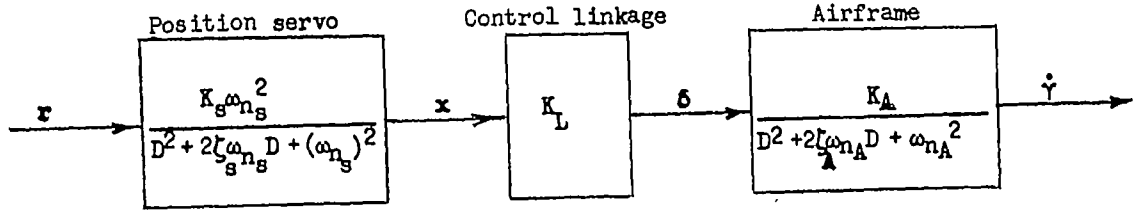

(b) Position-servo-actuated missile.

Figure 2.- Control-system block diagrams for a missile actuated by a torposervo and by a position-control-surface servo.

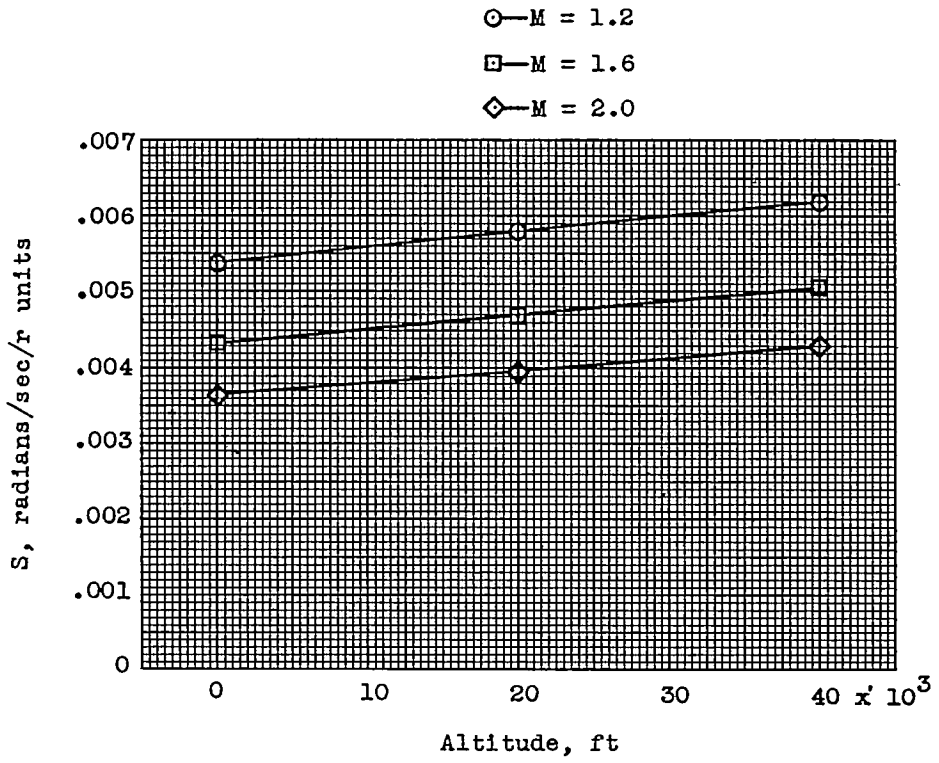

(a) Torque-servo-actuated airframe.

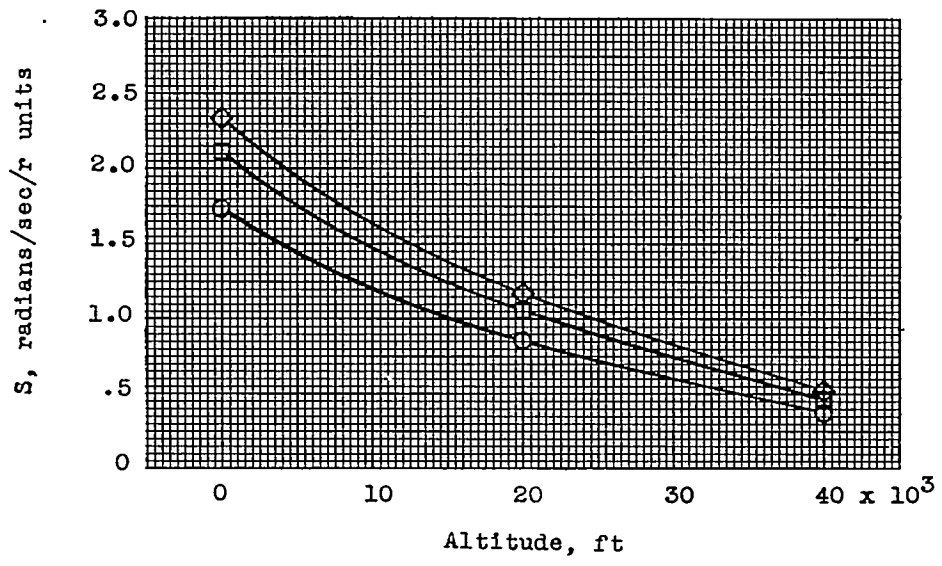

(b) Position-servo-actuated airframe.

Figure 3.- Plots of the static gain of a torque-servo- and position-servo-actuated missile showing the effect of Mach number and altitude for $SM = 0.564\bar{c}$ and $K_T = 1.0$.

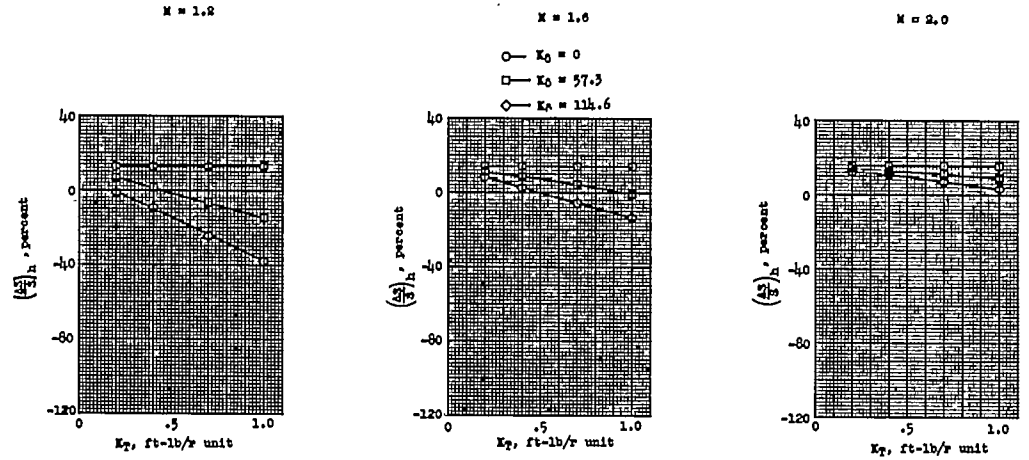

(a) SM = 0.094$\bar{c}$.

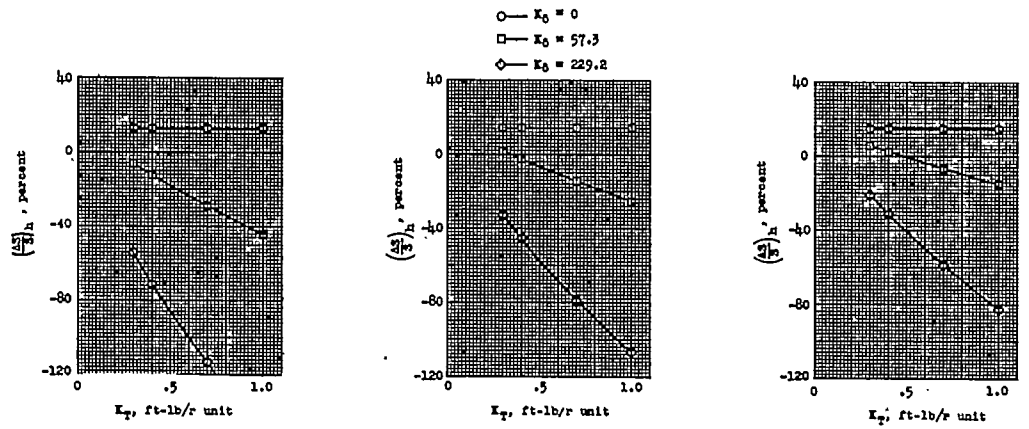

(b) SM = 0.564$\bar{c}$.

Figure 4.- Percentage variation of the static gain of the S torposervo-actuated missile for an altitude change from sea level to 40,000 feet.

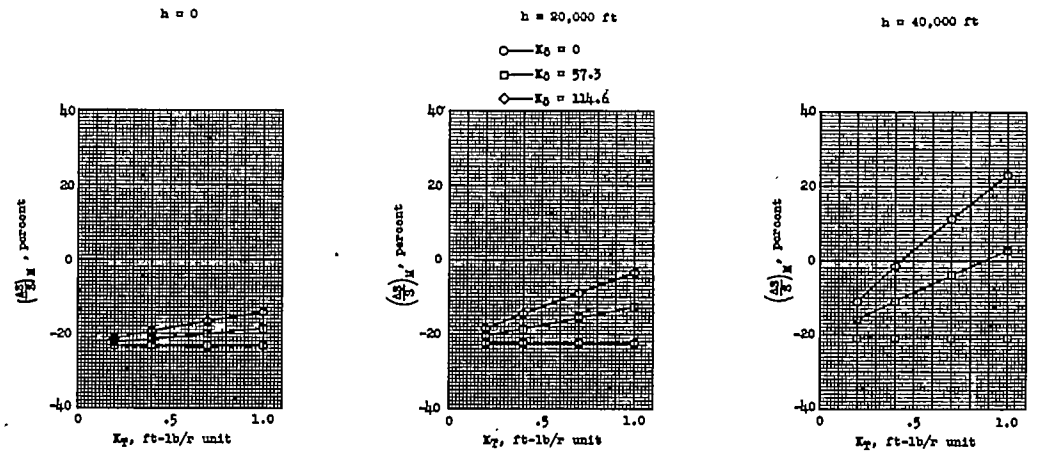

(a) SM = 0.094$\bar{c}$.

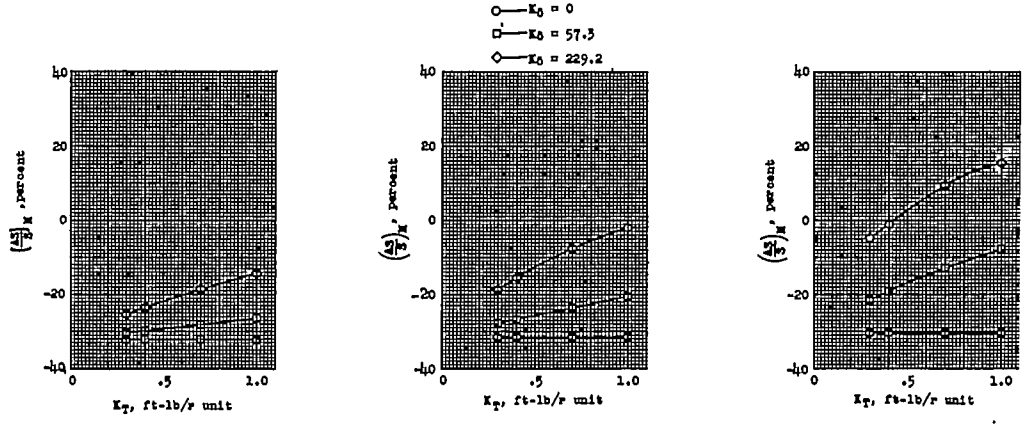

(b) SM = 0.564$\bar{c}$.

Figure 5.- Percentage variation of the static gain S of the torposervo-actuated missile for a Mach number change from 1.2 to 2.0.

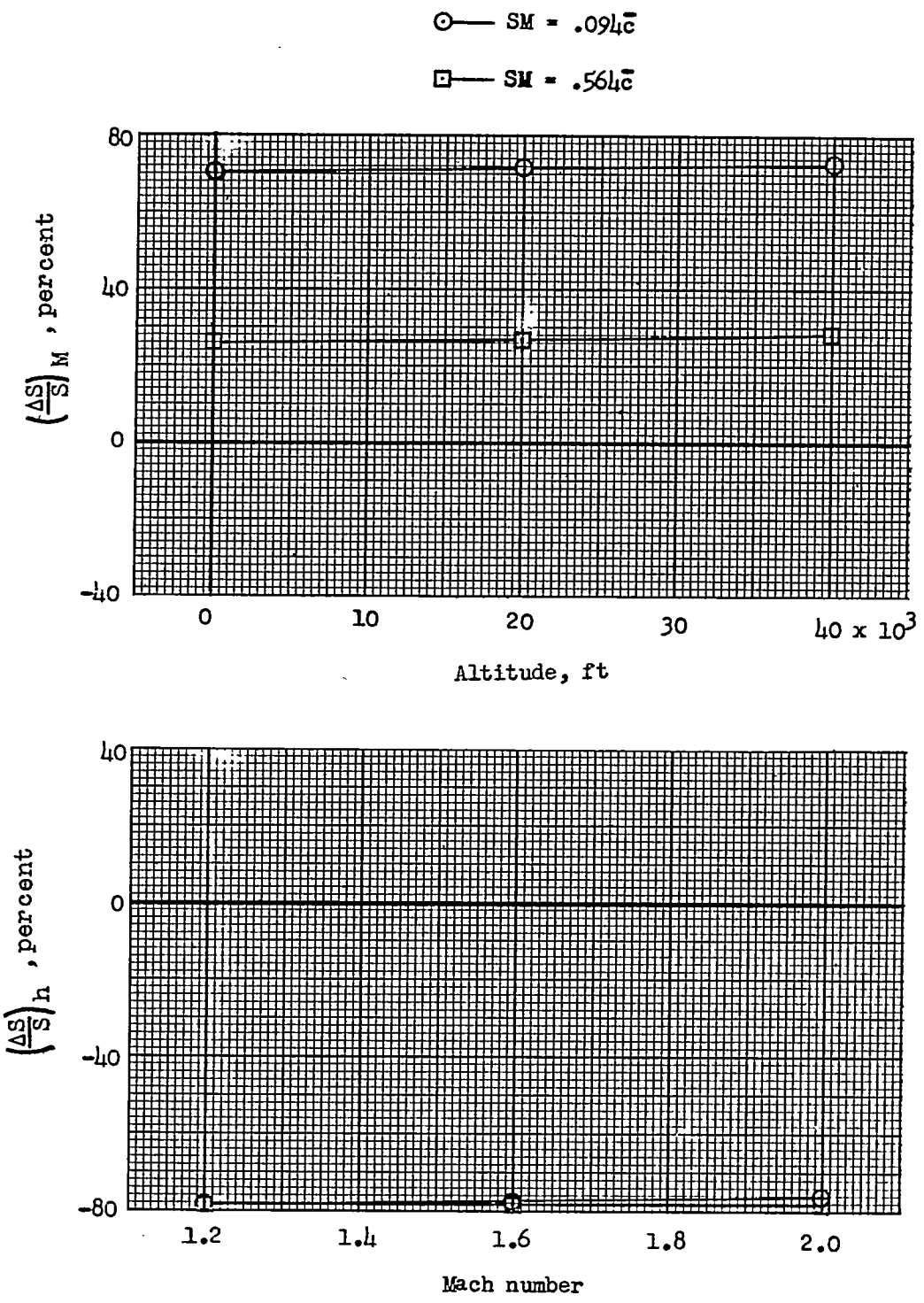

Figure 6.- Percentage variation static gain S of the position-servo-actuated missile for a change in Mach number from 1.2 to 2.0 and altitude from sea level to 40,000 feet.

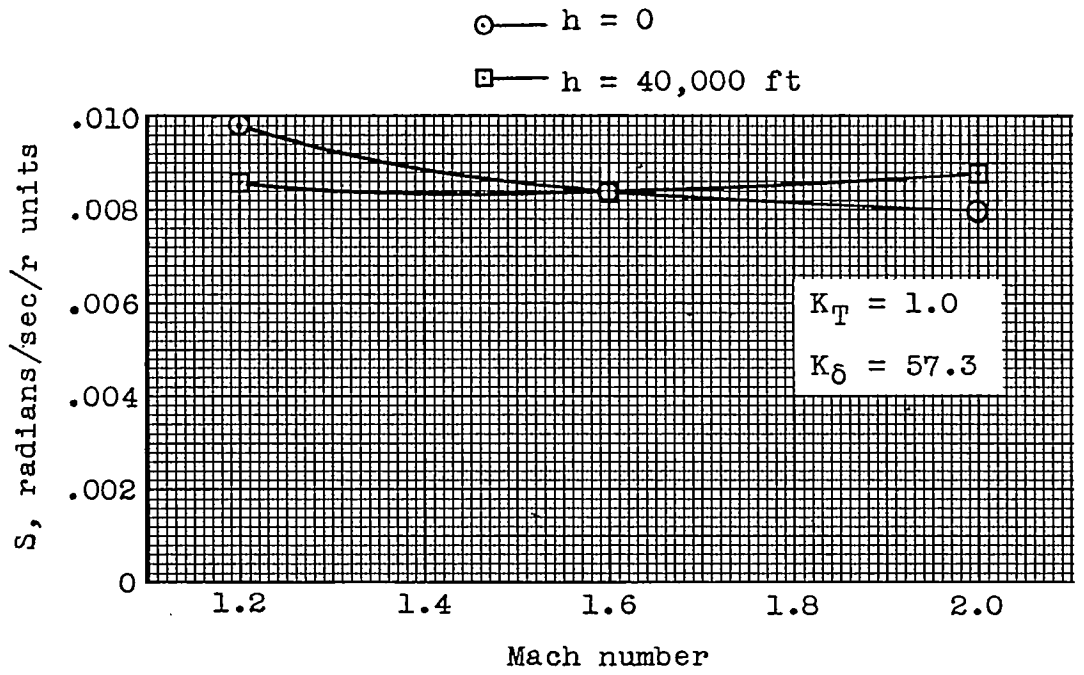

(a) K_T and K_δ adjusted for minimum Mach number variation.

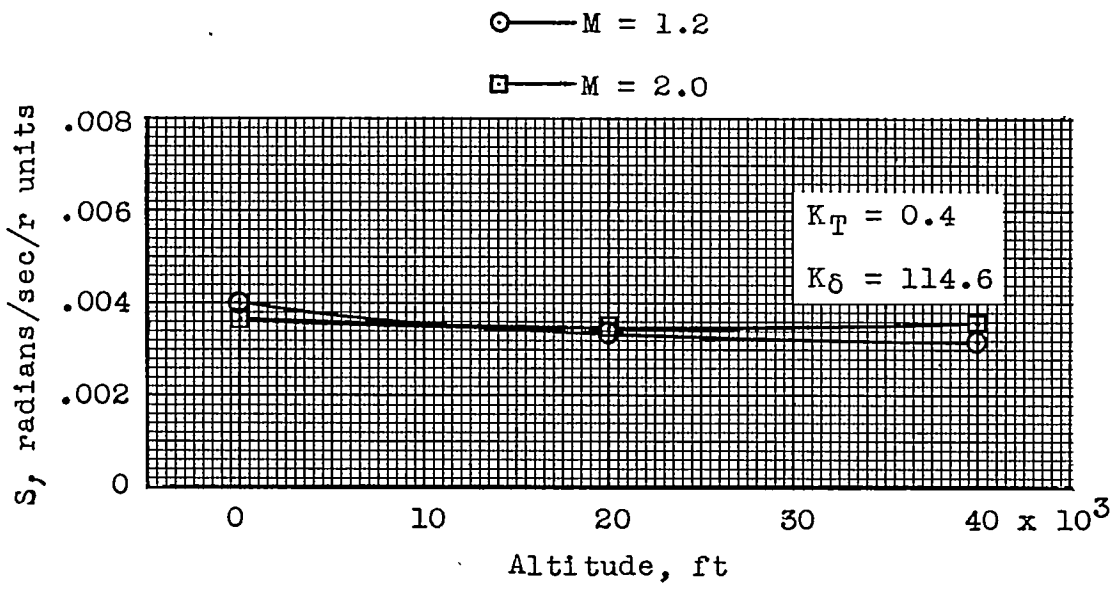

(b) K_T and K_δ adjusted for minimum altitude variation.

Figure 7.- Plots of the torposervo-system static gain against Mach number and altitude for the K_T and K_δ adjustment yielding minimum Mach number and altitude percentage variations for the small static margin airframe. SM = 0.094$\bar{c}$.

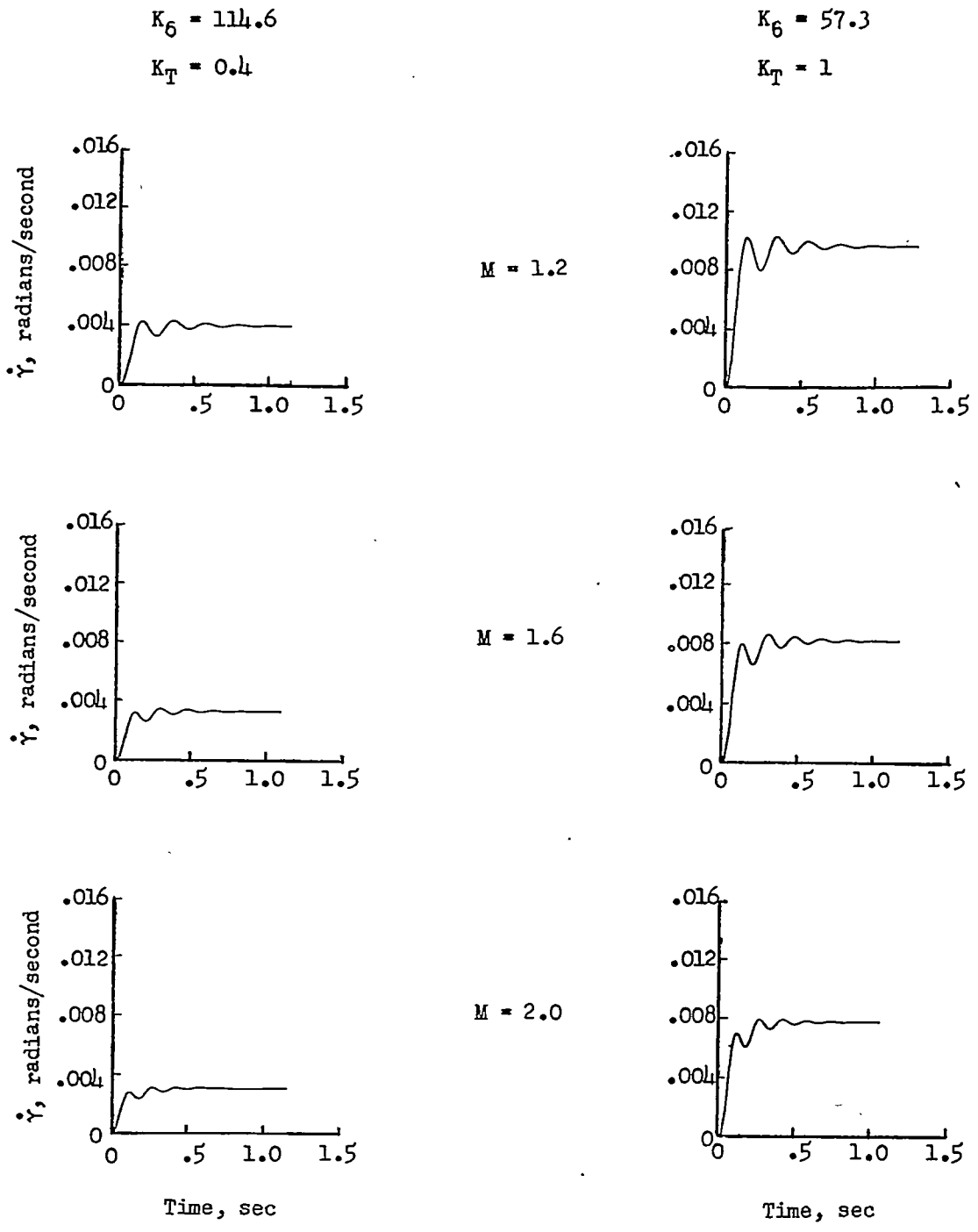

(a) Sea level.

Figure 8.- Transient responses of torposervo-actuated missile showing the time rate of change of flight-path angle subsequent to a unit step input signal r. SM = 0.094$\bar{c}$; $H_{\dot{\delta}}$ = -0.4 ft-lb/radian/second; τ = 0.1 second; I_R = 0.01 slug-ft^2.

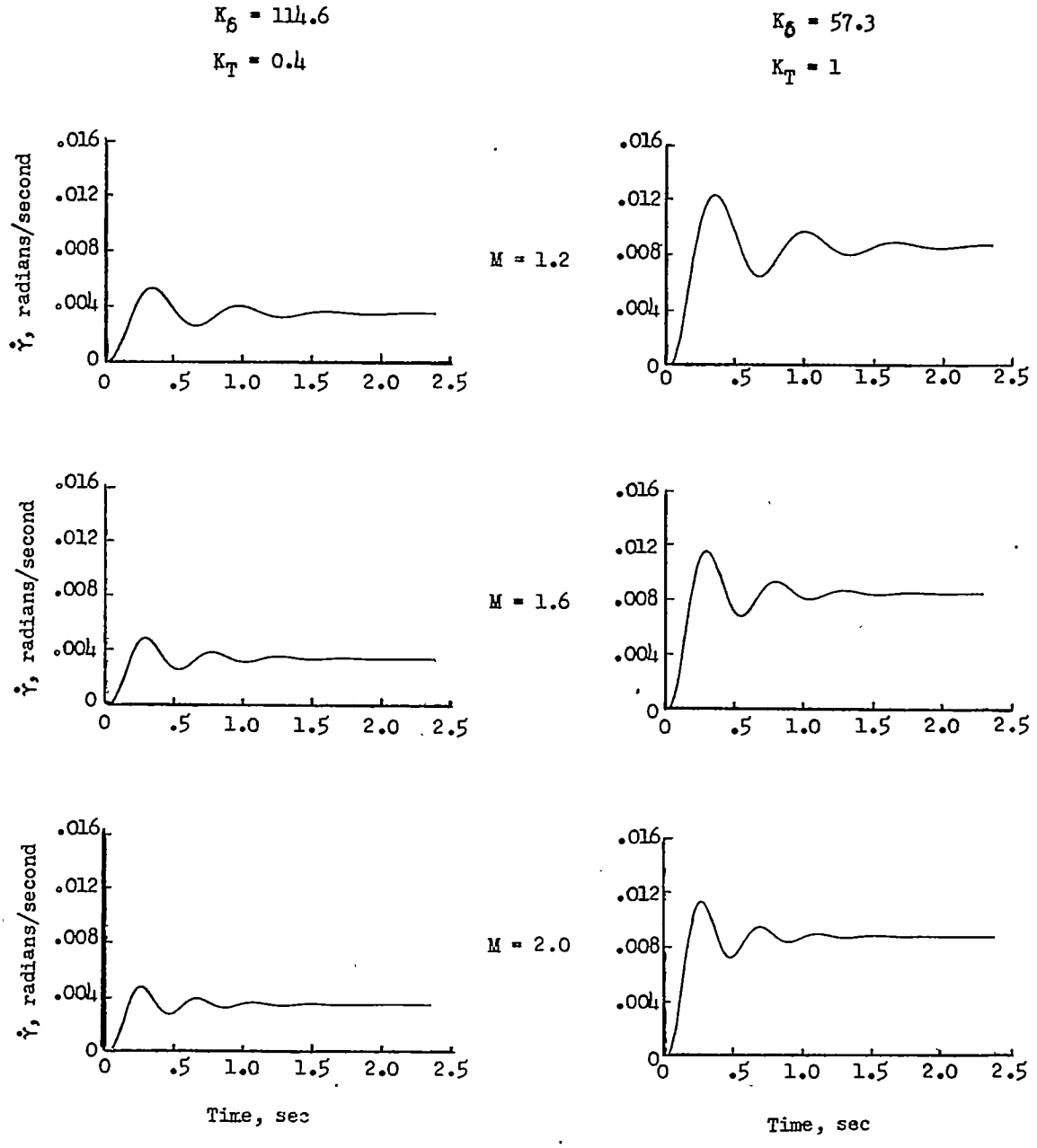

(b) 40,000 feet.

Figure 8.- Concluded.

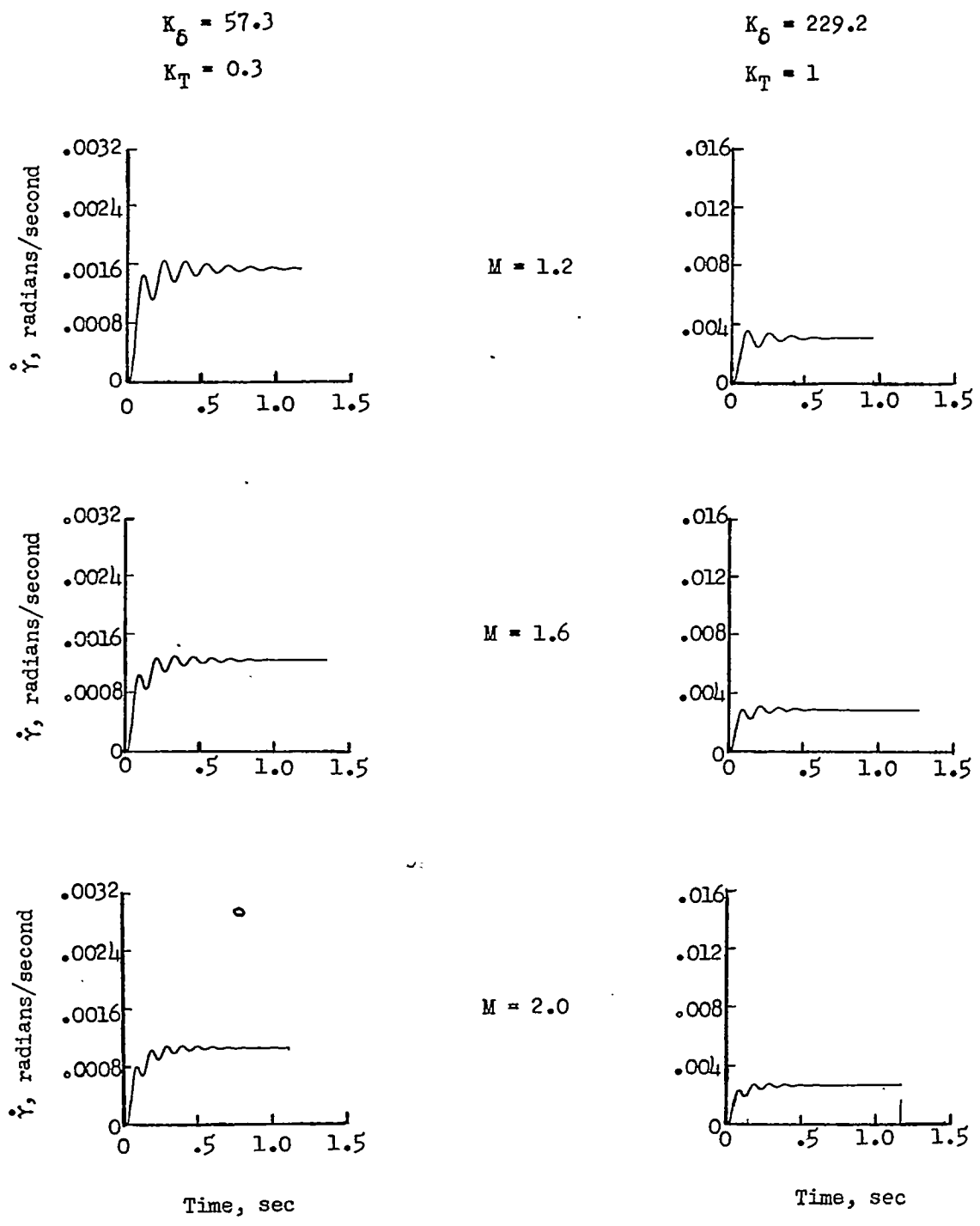

(a) Sea level.

Figure 9.- Transient responses of torposervo-actuated missile showing the time rate of change of flight-path angle subsequent to a unit step input signal r. SM = 0.564$\bar{c}$; $H_{\dot{\delta}}$ = -0.6 ft-lb/radian/second; τ = 0.1 second; I_R = 0.01 slug-ft^2.

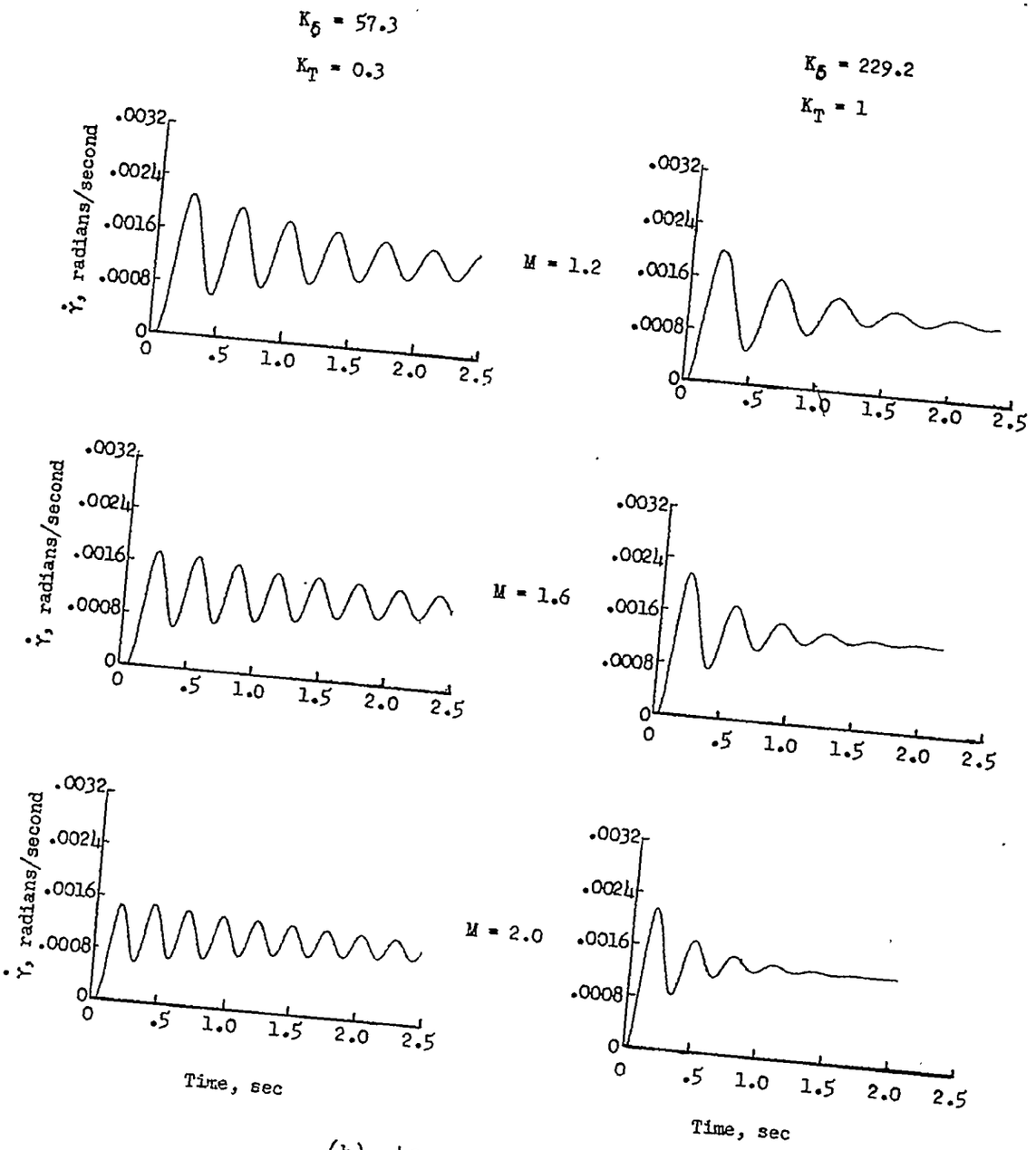

(b) 40,000 feet.

Figure 9.- Concluded.

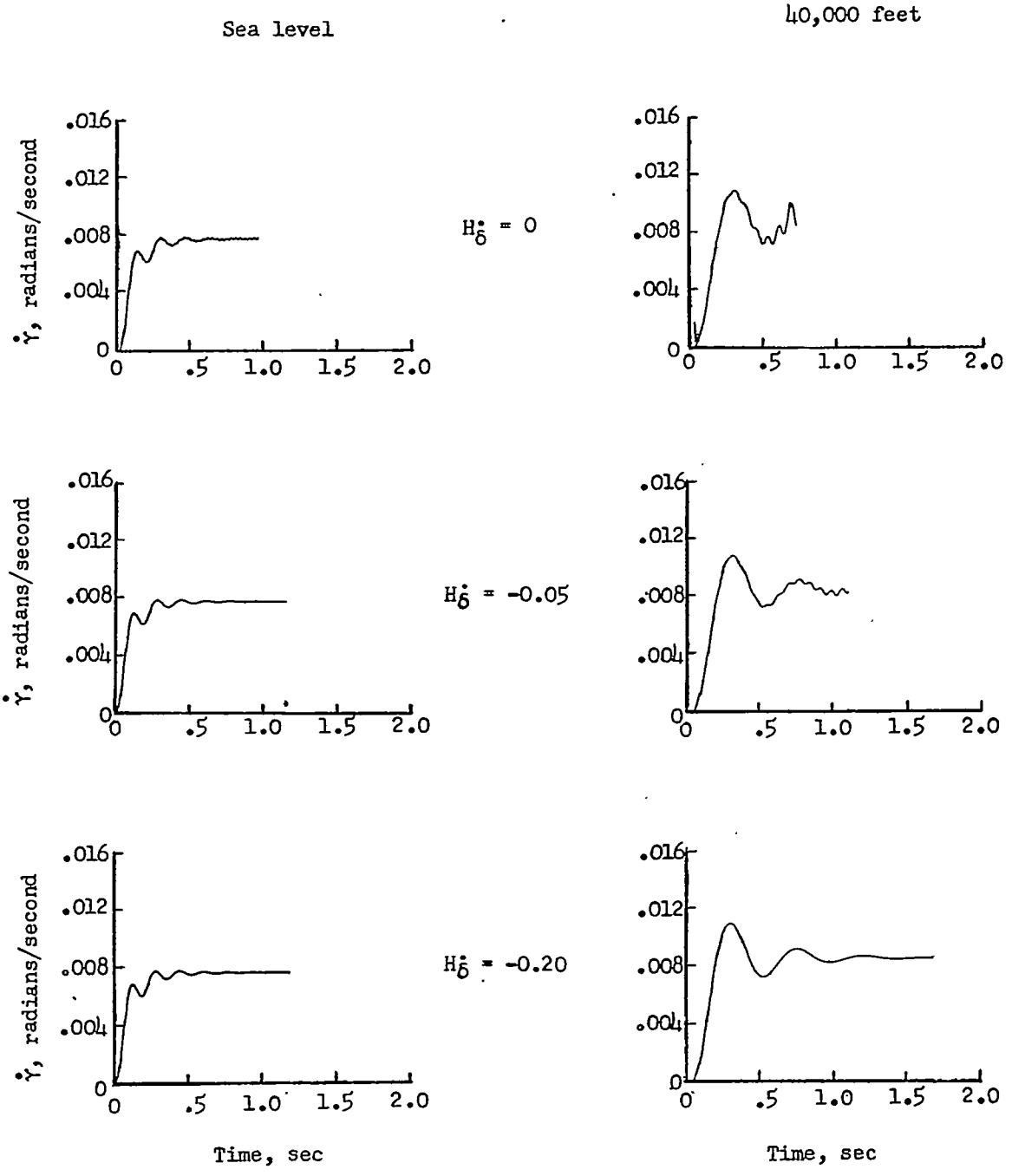

Figure 10.- Torposervo-system transient responses of the time rate of change of flight-path angle subsequent to a step input signal r showing the effect of control surface damping, $H_{\dot{\delta}}$. SM = 0.094$\bar{c}$; K_δ = 57.3 r units/radian; K_T = 1 ft-lb/r unit; τ = 0.1 second; I_R = 0.01 slug-ft^2; M = 2.0.

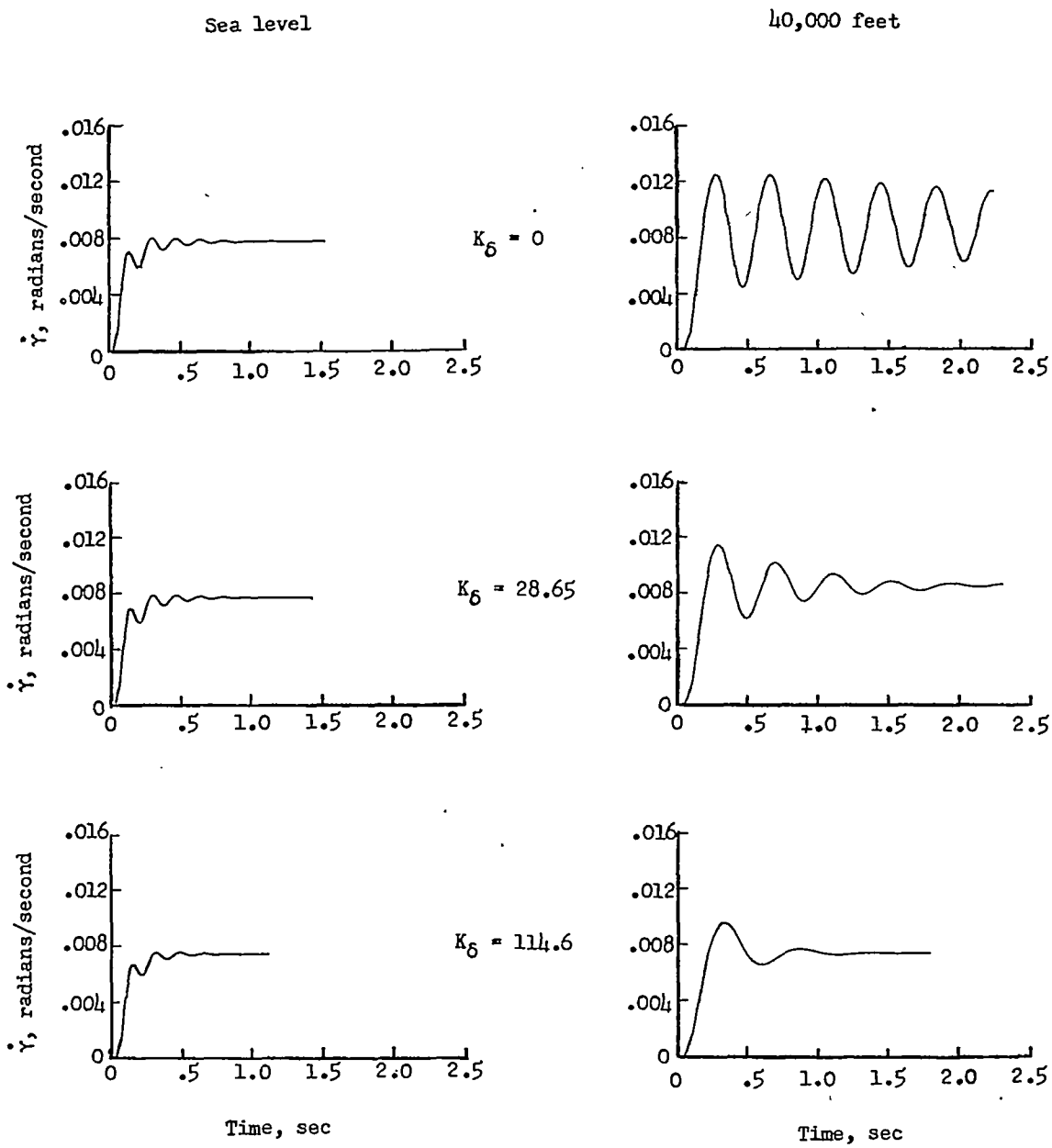

Figure 11.- Torposervo-system transient responses of the time rate of change of flight-path angle subsequent to a step input signal r showing the effect of position feedback, K_δ. $SM = 0.094\bar{c}$; $K_T = 1$ ft-lb/r unit; $H_{\dot{\delta}} = -0.4$ ft-lb/radian/second; $\tau = 0.1$ second; $I_R = 0.01$ slug-ft^2; $M = 2.0$.

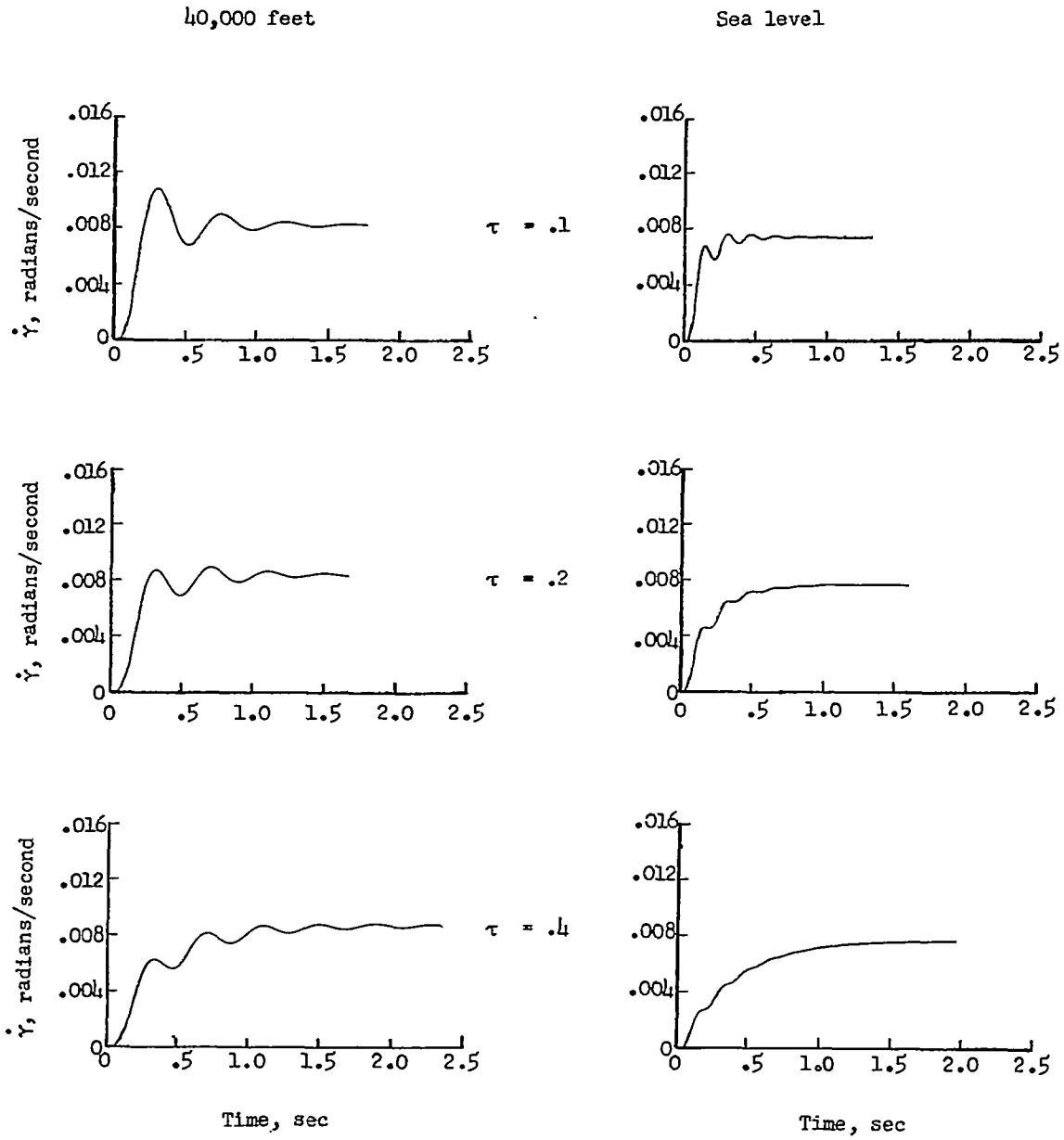

Figure 12.- Torposervo-system transient responses of the time rate of change of flight-path angle subsequent to a step input signal r showing the effect of servo time constant τ. SM = 0.094$\bar{c}$; K_δ = 57.3 r units/radian; K_T = 1 ft-lb/r unit; $H_{\dot{\delta}}$ = -0.4 ft-lb/radian/second; I_R = 0.01 slug-ft^2; M = 2.0.

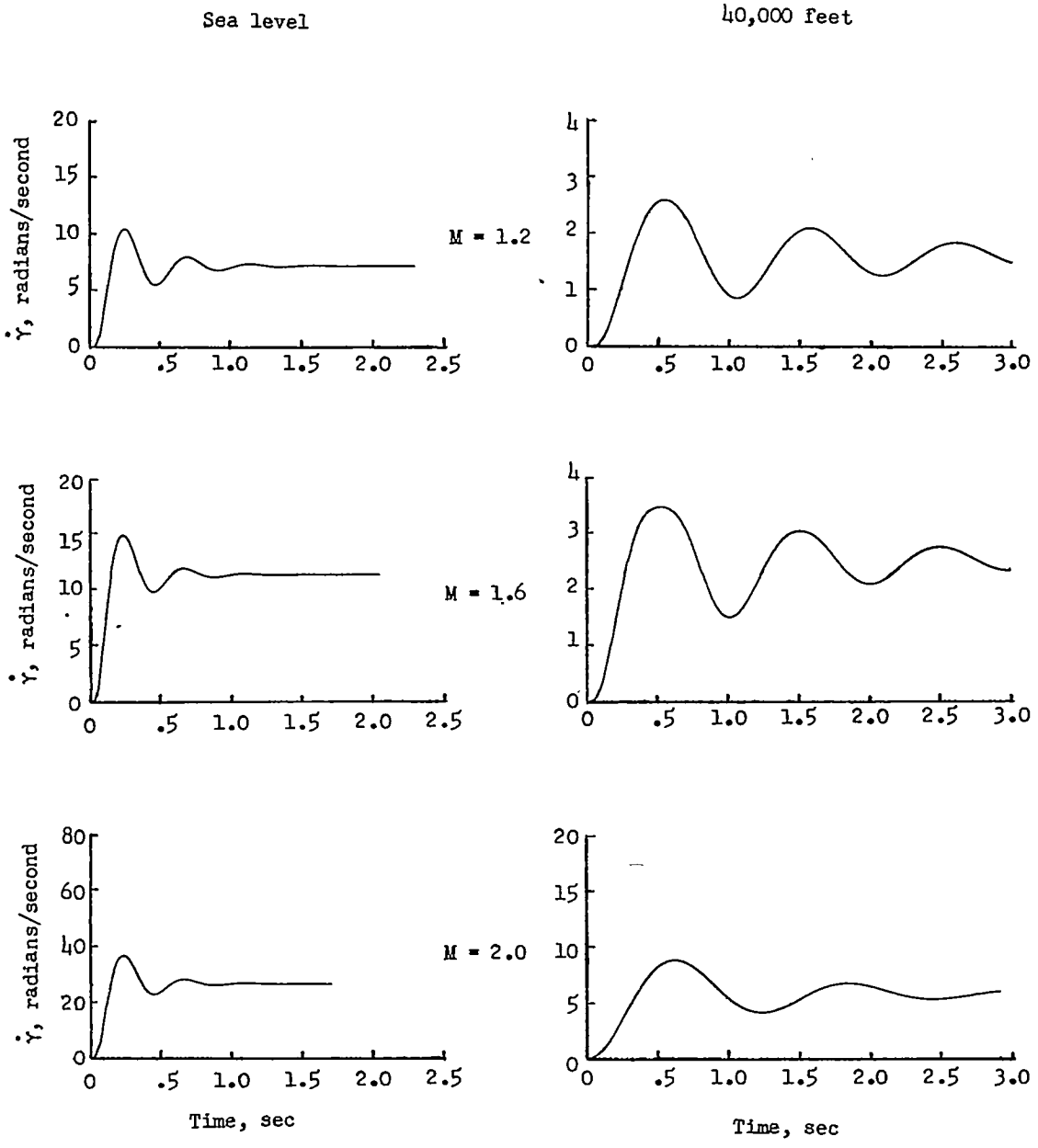

(a) SM = 0.094$\bar{c}$.

Figure 13.- Position-servo-system transient responses of the time rate of change of flight-path angle subsequent to a unit step input signal r showing the effect of Mach number, altitude, and static margin. $K_sK_L = 1.0$; $\zeta_s = 0.5$; $\omega_{n_s} = 60$.

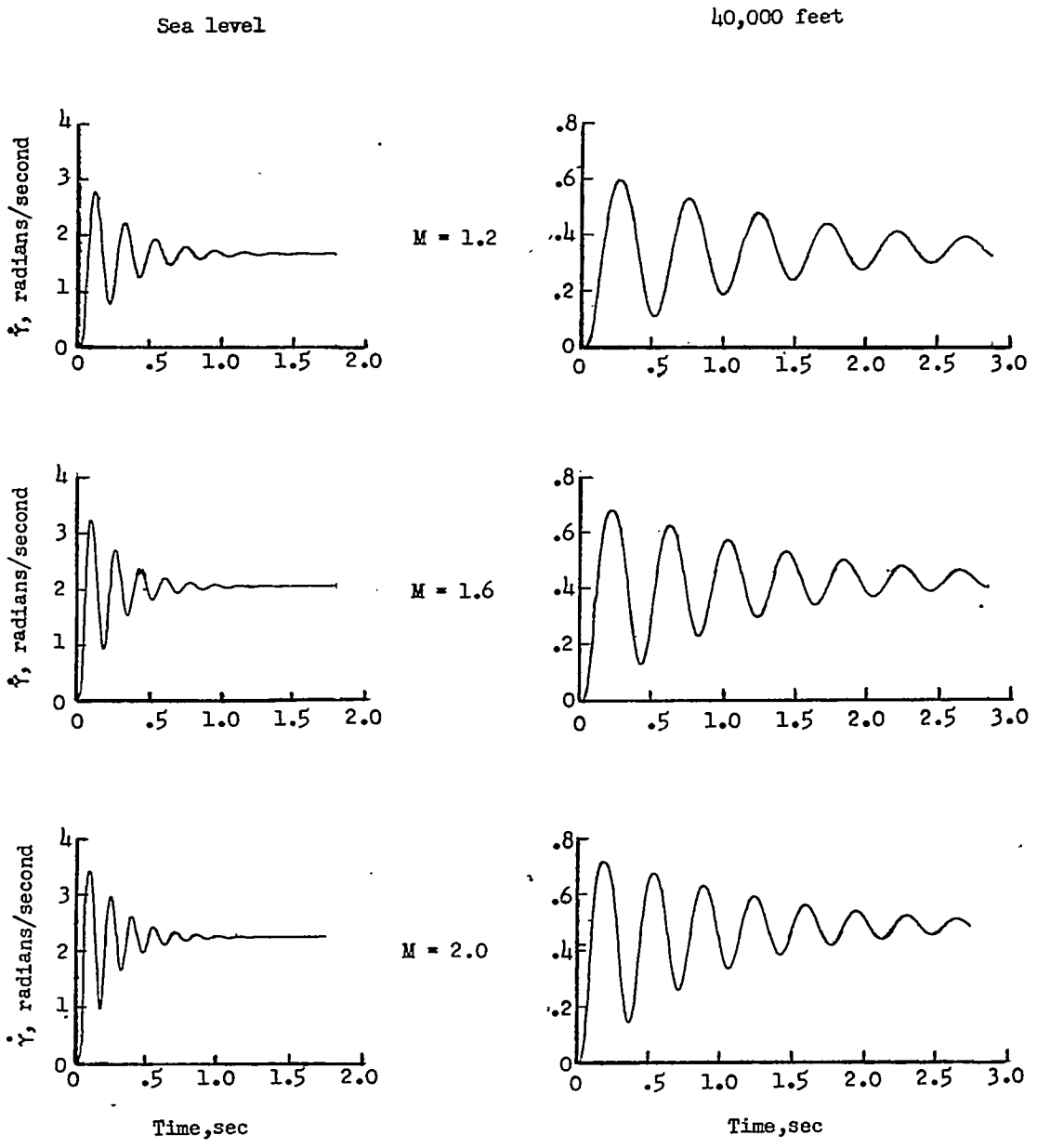

(b) SM = 0.564$\bar{c}$.

Figure 13.- Concluded.

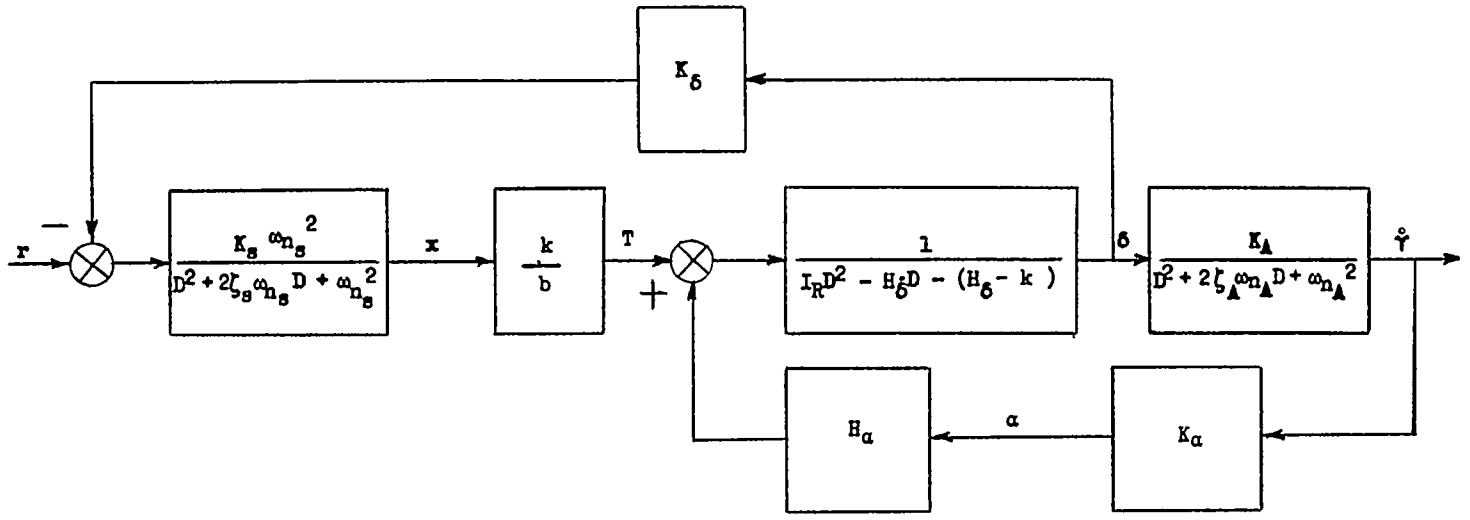

(a) Block diagram.

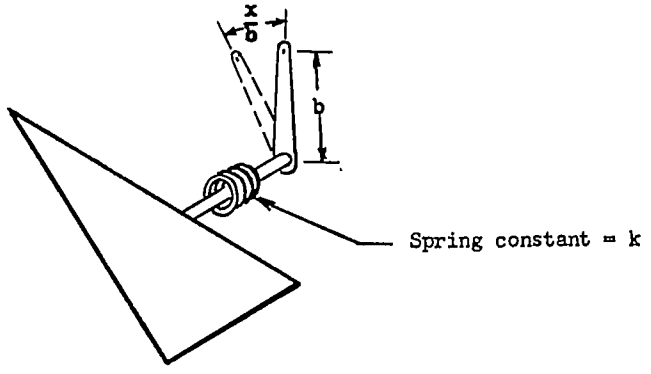

(b) Diagramatic sketch of control surface and spring.

Figure 14.- Block diagram and functional sketch of a missile actuated by a spring-position control-surface servo.

NACA - Langley Field, Va.

[redacted]

HADC
TECHNICAL LIBRARY
AFL 2811